Neural Comput & Applic (2015) 26:1005–1024
DOI 10.1007/s00521-014-1763-1

ORIGINAL ARTICLE

Prediction model for compressive strength of basic concrete mixture using artificial neural networks

Srđan Kostić · Dejan Vasović

Received: 6 April 2014 / Accepted: 16 October 2014 / Published online: 30 October 2014

Abstract In the present paper, we propose a prediction model for concrete compressive strength using artificial neural networks. In experimental part of the research, 75 concrete samples with various *w*/*c* ratios were exposed to freezing and thawing, after which their compressive strength was determined at different age, viz. 7, 20 and 32 days. In computational phase of the research, different prediction models for concrete compressive strength were developed using artificial neural networks with *w*/*c* ratio, age and number of freeze/thaw cycles as three input nodes. We examined three-layer feed-forward back-propagation neural networks with 2, 6 and 9 hidden nodes using four different learning algorithms. The most accurate prediction models, with the highest coefficient of determination ($R^2 > 0.87$), and with all of the predicted data falling within the 95 % prediction interval, were obtained with six hidden nodes using Levenberg–Marquardt, scaled conjugate gradient and one-step secant algorithms, and with nine hidden nodes using Broyden–Fletcher–Goldfarb–Shannon algorithm. Further analysis showed that relative error between the predicted and experimental data increases up to acceptable $\approx$15 %, which confirms that proposed ANN models are robust to the consistency of training and validation output data. Accuracy of the proposed models was further verified by low values of standard statistical errors. In the final phase of the research, individual effect of each input parameter was examined using the global sensitivity analysis, whose results indicated that *w*/*c* ratio has the strongest impact on concrete compressive strength.

Keywords Concrete · Compressive strength · Artificial neural network · Robustness · Global sensitivity analysis

S. Kostić (✉)
Department of Geology, University of Belgrade Faculty of Mining and Geology, Đušina 7, 11000 Belgrade, Serbia
e-mail: srdjan.kostic@rgf.bg.ac.rs

S. Kostić
Faculty of Mining, University of Banja Luka, Save Kovačevića bb, 79000 Prijedor, Republic of Srpska, Bosnia and Herzegovina

D. Vasović
Department of Architectural Technologies, University of Belgrade Faculty of Architecture, 11000 Belgrade, Serbia

1 Introduction

Rapid development of new technologies, as well as the increase in production of synthetic ingredients, enables the constructors to create and use different types of concrete, depending on the type of object, possible external static and dynamic forces and surrounding environment. Increasing demands for higher and stronger buildings, together with more complicated architectural designs, seek concrete mixtures of higher quality, which are typically obtained by including a certain amount of the appropriate additive. Depending on the property which is to be improved, concrete is usually mixed with different plasticizers and superplasticizers, ground granulated blast furnace slag, pozzolanic ash, as well as fly ash or silica fume. Hence, as it could be seen, there is a variety of factors that could affect the ultimate characteristic of the concrete. Nevertheless, its physical and mechanical properties are still predetermined by the three main ingredients: water, cement, and aggregates, which are typically represented by the *w*/*c* ratio, physical, mechanical and chemical properties of cement and by the aggregate granulometric structure. It is this basic concrete mixture, without additives, that is examined in present paper, in order to obtain a reliable model for prediction of concrete

compressive strength. Prediction models are very useful in laboratory testing, since they optimize experimental process by providing an optimal minimum number of probes for analyzing a specific property of concrete mixture. Several different prediction models have been developed, which are frequently used for estimating the compressive strength, as the most important engineering property of the concrete. First of them is based on linear and nonlinear regression analysis, commonly using the maturity concept [1–4], as well as the combination of input variables, water, cement and aggregates [5, 6]. Second approach uses the adaptive network-based fuzzy inference system [7, 8], while third approach relies on fuzzy logic techniques [9–12].

Apart from the aforementioned models, in recent years, artificial neural networks (ANN) have been used for estimating different concrete properties, such as drying shrinkage [13], concrete durability [14], ready mixed concrete delivery [15], compressive strength of normal and high-performance concrete [16–23], workability of concrete with metakaolin and fly ash [24], mechanical behavior of concrete at high temperatures [25] and long-term effect of fly ash and silica fume on concrete compressive strength [26]. The main advantage of ANN approach over the other computational methods lies in the fact that ANN automatically manages to detect the multivariable interrelationships. From an engineering point of view, this modeling method results in a concrete mix proportion with the lesser number of trials, cost and time.

In the present paper, we develop ANN models for prediction of concrete compressive strength based on the results of a series of experiments. The obtained model would be able to reproduce the experimental results and to approximate the results in other experiments through its generalization capability. The present research is focused on compressive strength of basic concrete mixture, depending on three main factors: *w/c* ratio, age and exposure to freezing and thawing.

The paper is organized as follows. Material properties and testing procedure are described in Sect. 2, while experimental results are provided in Sect. 3. The obtained results of ANN modeling are presented and compared with experimental data in Sect. 4, while their performance is further evaluated in Sect. 5. Results of global sensitivity analysis are presented and discussed in Sect. 6. A brief review on the obtained results is given in the final section, together with suggestions for further research.

2 Laboratory testing

2.1 Properties of cement

The examined concrete specimens were made of CEM I normal Portland cement (PC 42.5 N/mm^2), manufactured by Lafarge BFC (Serbia), with specific gravity $\rho = 3.10$ g/cm^3, and with the initial and final setting times of 2 h and 30 min and 3 h and 30 min, respectively. Blaine specific surface area of cement was 3,450 cm^2/g. Physical and mechanical properties of cement and its chemical composition were determined by Institute for testing of materials—IMS Serbia (Tables 1, 2).

2.2 Properties of aggregate

Concrete mixture included natural river aggregate. Maximum nominal size of gravel was 16 mm with 5 % of the oversized particles (Table 3). The water absorption was 1.5 %, and its relative density at saturated surface dry condition (SSD) was 2.72 g/cm^3. The water absorption value of sand was 2.0 %, and its relative density at SSD condition was 2.69 g/cm^3.

2.3 Preparation of concrete specimens

Concrete was made in a laboratory counter-current concrete mixer of "'Eiric" type. Cubic concrete samples (100 × 100 mm) were made and examined according to the national standard SRPS [27, 28]. Mixing period was 3 min for all mixtures. Casting was performed at a vibrating table until a complete consolidation was achieved. Consistency of the fresh concrete was measured by applying the slump test [29], Vebe test [30] and flow test [31] (Table 4).

2.4 Test procedure

After the concrete was casted in metal moulds, samples were left at room temperature (20 ± 2 °C) with relative humidity of 90–95 %. Concrete samples were demoulded after 24 h and soaked in water at the same temperature (20 °C) for the next 6 days. At the seventh day, four out of eight series of the concrete samples were exposed to freezing and thawing. Compressive strength was determined after 50 and 100

Table 1 Physical and mechanical properties of cement

Property	Value	
Specific gravity (g/cm^3)	3.10	
Specific surface (cm^2/g)	3,450	
Setting time initial (min)	150	
Setting time final (min)	210	
Volume expansion (mm)	0.50	
Compressive strength (MPa)	2 days	28 days
	15.1	49.5
Flexural strength (MPa)	2 days	28 days
	3.5	8.7

Table 2 Chemical composition of cement

Oxide	SiO_2	Al_2O_3	Fe_2O_3	CaO	MgO	SO_3	CaO	Na_2O	K_2O
Cement	20.58	6.04	2.54	58.79	2.66	3.08	2.16	0.29	0.76

Table 3 Grading of the mixed aggregate

Sieve size (mm)	0.09	0.13	0.25	0.5	1	2	4	8	11.2	16	22.4
0/4 (% passed)	1	4	21	67	76	84	94	100	100	100	100
4/8 (% passed)	0	0	0	0	0	1	12	97	100	100	100
8/16 (% passed)	0	0	0	0	0	0	0	19	67	95	100

Table 4 Concrete mixture proportions and consistency

Sample no.	*C* (kg)	*A* (kg)	*W/C*	Slump (cm)	Vebe (s)	Flow (cm)
A1	350	1,930	0.45	0.5	8	23
A2	350	1,930	0.40	0	11	28
A3	350	1,930	0.50	4.5	4	35
A4	350	1,930	0.55	15.5	2	54
A5	350	1,930	0.35	0	27	35

cycles (one cycle lasted for 4 h in environmental chamber at -20 ± 2 °C and 4 h soaked in water at 20 ± 2 °C) after 7, 20 and 32 days. Measured strength was compared with the strength of the control group of specimens, continuously cured in water at 20 ± 2 °C, which were not exposed to freezing and thawing, also after 7, 20 and 32 days [32]. These ages were chosen so as to fall on a working day. Moreover, it is a common practice to observe a development of concrete strength after 1, 3, 5, 7, 14, 21 and 28 days, in order to capture the relative gain of strength in time [33]. Differences between the observed strength after 20 and 21 days, or after 28 and 32 days, are not higher than few percentages [33]. The compressive strength and bulk density of the hardened concrete were tested according to the national SRPS standard [34]. Compressive strength measurements were carried out using "Amsler" hydraulic press with capacity of 2,000 kN and with loading rate of 0.4 MPa/s.

3 Experimental results

Results of the performed testing of 75 concrete samples are given in Table 5. For each composition of concrete mixture, compressive strength of specimens was determined after three probes, in order to reduce the measurement error. Testing results imply that the maximum difference between the largest and smallest value of compressive strength for samples of the same composition (and exposed to the equal number of freezing/thawing cycles) is in the range of 10 %, except for the following group of specimens: A5-4 → A5-6, A3-7 → A3-9, A1-10 → A1-12, A2-10 → A2-12, A1-13 → A1-15, A2-13 → A2-15, A5-13 → A5-15, where the difference between the measured strengths increases even up to >20 %. However, despite such relatively high contrasts, all the experimental results were used for ANN modeling, in order to examine the robustness of the prediction models to the consistency of training and validation output data.

Regarding the impact of particular concrete ingredients, the obtained results clearly indicate the strong influence of *w/c* ratio on concrete compressive strength. Samples of concrete with lower *w/c* ratio show higher compressive strength, determined by the aggregate grading and amount of cement in the mixture. On the other hand, exposure to freeze and thawing decreases the concrete strength, especially at higher *w/c* ratios.

4 Development of prediction model

Prediction model for concrete compressive strength was developed using three-layer back-propagation feed-forward artificial neural networks, with *w/c* ratio, age and the number of freeze/thaw cycles as input parameters, whereas compressive strength was considered as a single output unit (Table 6). Similar approach was already used in [6, 35–37].

Following the suggestion of Rumelhart et al. [38], Lippmann [39] and Sonmez et al. [40], we chose ANN

Table 5 Compressive strength of concrete—experimental results

Sample	*W/C*	*t* (days)	*F/T*	σ_p (MPa)	Sample	*W/C*	*t* (days)	*F/T*	σ_p (MPa)
A1-1	0.45	32	100	55.00	A3-9	0.50	32	0	40.00
A1-2	0.45	32	100	54.00	A4-7	0.55	32	0	38.00
A1-3	0.45	32	100	51.00	A4-8	0.55	32	0	37.60
A2-1	0.40	32	100	45.60	A4-9	0.55	32	0	37.60
A2-2	0.40	32	100	49.25	A5-7	0.35	32	0	49.00
A2-3	0.40	32	100	48.00	A5-8	0.35	32	0	48.80
A3-1	0.50	32	100	47.60	A5-9	0.35	32	0	50.50
A3-2	0.50	32	100	46.00	A1-10	0.45	20	0	49.60
A3-3	0.50	32	100	46.20	A1-11	0.45	20	0	44.55
A4-1	0.55	32	100	37.40	A1-12	0.45	20	0	44.80
A4-2	0.55	32	100	36.30	A2-10	0.40	20	0	47.50
A4-3	0.55	32	100	38.40	A2-11	0.40	20	0	38.50
A5-1	0.35	32	100	50.40	A2-12	0.40	20	0	44.00
A5-2	0.35	32	100	53.50	A3-10	0.50	20	0	41.00
A5-3	0.35	32	100	49.00	A3-11	0.50	20	0	41.00
A1-4	0.45	20	50	49.00	A3-12	0.50	20	0	41.00
A1-5	0.45	20	50	48.60	A4-10	0.55	20	0	32.00
A1-6	0.45	20	50	45.20	A4-11	0.55	20	0	32.60
A2-4	0.40	20	50	50.80	A4-12	0.55	20	0	29.70
A2-5	0.40	20	50	50.90	A5-10	0.35	20	0	50.20
A2-6	0.40	20	50	51.10	A5-11	0.35	20	0	49.60
A3-4	0.50	20	50	38.00	A5-12	0.35	20	0	49.20
A3-5	0.50	20	50	39.10	A1-13	0.45	7	0	35.00
A3-6	0.50	20	50	40.20	A1-14	0.45	7	0	28.00
A4-4	0.55	20	50	30.80	A1-15	0.45	7	0	35.50
A4-5	0.55	20	50	30.80	A2-13	0.40	7	0	36.40
A4-6	0.55	20	50	29.70	A2-14	0.40	7	0	41.00
A5-4	0.35	20	50	50.40	A2-15	0.40	7	0	41.50
A5-5	0.35	20	50	43.80	A3-13	0.50	7	0	31.20
A5-6	0.35	20	50	50.40	A3-14	0.50	7	0	32.40
A1-7	0.45	32	0	52.50	A3-15	0.50	7	0	34.00
A1-8	0.45	32	0	50.50	A4-13	0.55	7	0	21.60
A1-9	0.45	32	0	49.80	A4-14	0.55	7	0	21.40
A2-7	0.40	32	0	48.90	A4-15	0.55	7	0	22.50
A2-8	0.40	32	0	45.60	A5-13	0.35	7	0	40.00
A2-9	0.40	32	0	48.80	A5-14	0.35	7	0	37.10
A3-7	0.50	32	0	36.70	A5-15	0.35	7	0	42.20
A3-8	0.50	32	0	33.30					

t denotes the age of concrete, *F/T* number of freeze/thaw cycles, σ_p compressive strength of concrete

model with one hidden layer, while the number of hidden nodes was determined using heuristics summarized by Sonmez et al. [40]. As it is clear from Table 7, the number of nodes that may be used in hidden layer varies between 1 and 9. In the present study, we examined ANN models with 2, 6 and 9 hidden neurons in order to establish the most effective ANN architecture.

In all the examined cases, the total data set has been divided as following: 60 % for training (45 recordings), 15 % for validation (11 recordings) and 25 % for testing (19 recordings), which corresponds well with the suggestion of Looney [41], who proposed 25 % for testing, and with recommendation made by Nelson and Illingworth [42] who supported the idea of 20–30 % of data

Table 6 Input–output parameters for the ANN training and their range

Type of data	Parameter	Range
Inputs	*w/c* ratio (%)	0.35–0.55
	Age (days)	7–32
	Number of freeze/thaw cycles	0–100
Output	Compressive strength (MPa)	21.4–55

Table 7 Different heuristics used for the number of nodes in hidden layer (N_i number of input nodes, N_0 number of output nodes)

Heuristic	Calculated number of nodes for this study
$\leq 2 \times N_i + 1$	≤ 7
$3 \times N_i$	9
$(N_i + N_0)/2$	2
$\frac{2+N_0 \times N_i + 0.5N_0 \times \left(N_0^2 + N_i\right) - 3}{N_i + N_0}$	1
$2N_i/3$	2
$\sqrt{(N_i + N_0)}$	2
$2N_i$	6

Summary of the heuristics is given in [40]

for testing. ANN training was performed using the Matlab Neural Network toolbox [43], with four different learning algorithms: Levenberg–Marquardt, scaled conjugate gradient, one-step-secant back-propagation and Broyden–Fletcher–Goldfarb–Shannon (BFGS) quasi-Newton back-propagation. Results were obtained for random initial conditions and sampling.

The proposed ANN architectures were trained using combinations of the number of hidden nodes defined above. Since input parameters have different units of measure, scaling of their values was necessary, using the following relation:

$$\text{scaled value} = (\text{max.value} - \text{unscaled value})/(\text{max.value} - \text{min.value}) \quad (1)$$

In this way, values of all the input and output units were scaled in the range [0, 1].

4.1 Levenberg–Marquardt (LM) learning algorithm

LM learning algorithm is commonly considered as the fastest method for training moderate-sized feed-forward neural networks [44, 45], and it is the first choice for solving the problems of supervised learning, which is the case in the present analysis. As an activation function, we use sigmoid function which has been typically implemented in previous studies [39].

In order to create a prediction model with most accurate response, we developed three artificial neural networks with 2, 6 and 9 hidden neurons. The possibility of overfitting was excluded by confirming that any increase in accuracy over the training data set yields rise in accuracy over a validation data set. In the present study, mean-squared error (MSE) saturates with the increase of epochs for training and validation data for all three examined cases with different number of hidden neurons (Fig. 1).

Comparison of prediction results with experimental data for training, validation and testing sets, using ANNs with 2, 6 and 9 hidden nodes, is given in Fig. 2. It is clear that the ANN model with six hidden nodes has the highest coefficient of determination ($R^2 \approx 0.941$) for testing set, approximately the same value of R^2 for training and validation sets and with statistically small value of standard error, SE = 2.260, meaning that the average distance of the data points from the fitted line is 2.26 MPa. In other words, this means that all of predicted data fall within the 95 % prediction interval, which confirms the precision of the proposed model. A review of the experimental and predicted values of concrete compressive strength, including the absolute and relative prediction errors for ANN with six hidden nodes, is given in Table 8. Analysis of the error distribution for testing set shows that relative prediction errors are within the acceptable range of measurement results, up to ≈ 15 %.

4.2 Scaled conjugate gradient (SCG) learning algorithm

SCG learning algorithm belongs to the class of conjugate gradient optimization methods which are well suited to handle the large-scale problems in an effective way [46]. This method represents one of the four most commonly used algorithms of this group, besides Fletcher–Reeves Update, Polak–Ribiére Update and Powell–Beale Restarts algorithm. Each of these conjugate gradient algorithms requires a line search at every iteration step, which is computationally expensive, since the network response to all training inputs has to be computed several times for each search. The SCG algorithm was designed to avoid this time-consuming procedure, by combining the model-trust region approach (used in LM algorithm) with the conjugate gradient algorithm [47].

As in the previous case of LM algorithm, change of MSE with the increase of number of epochs was examined for training, validation and testing sets, using different

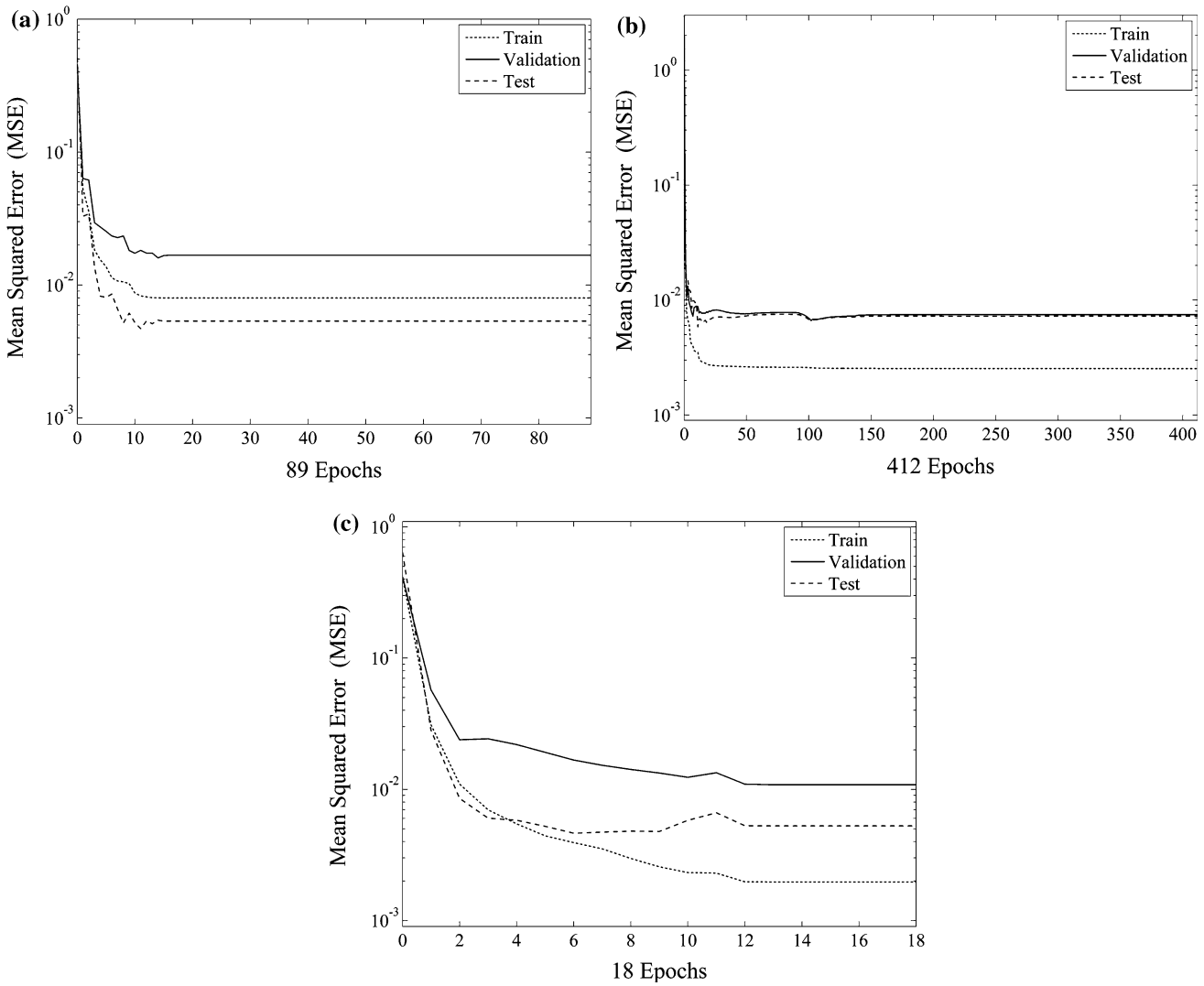

Fig. 1 MSE versus the number of epochs for training, validation and testing sets, using artificial neural networks with: **a** 2, **b** 6 and **c** 9 hidden nodes. MSE saturates with the increase of training epochs for both training and validation sets, excluding the possibility of overfitting

number of hidden nodes (Fig. 3). The analysis showed that training set errors and validation set errors have similar properties, confirming the absence of overfitting.

Comparison of prediction results with experimental data for training, validation and testing sets, using ANNs with 2, 6 and 9 hidden nodes, is given in Fig. 4. ANN model with six hidden nodes has the highest coefficient of determination ($R^2 \approx 0.877$) for testing set, approximately the same value of R^2 for validation set and with statistically small value of standard error, SE = 2.495, meaning that all of the predicted data fall within the 95 % prediction interval, which confirms the precision of the proposed model. A slight decrease of R^2 between the training and validation sets does not affect the obtained results significantly, since standard error indicates that predicted data fall within the 95 % prediction interval in both cases (SE = 2.062 and 2.756, respectively). Analysis of the error distribution for training set (for ANN with six hidden nodes) shows that relative prediction errors are in the range up to ≈15 % (Table 9).

4.3 Broyden–Fletcher–Goldfarb–Shannon (BFGS) quasi-Newton back-propagation learning algorithm

BFGS algorithm is considered as one of the best quasi-Newton's techniques that uses a local quadratic approximation of the error function and employs an approximation of the inverse of the Hessian matrix to update the weights,

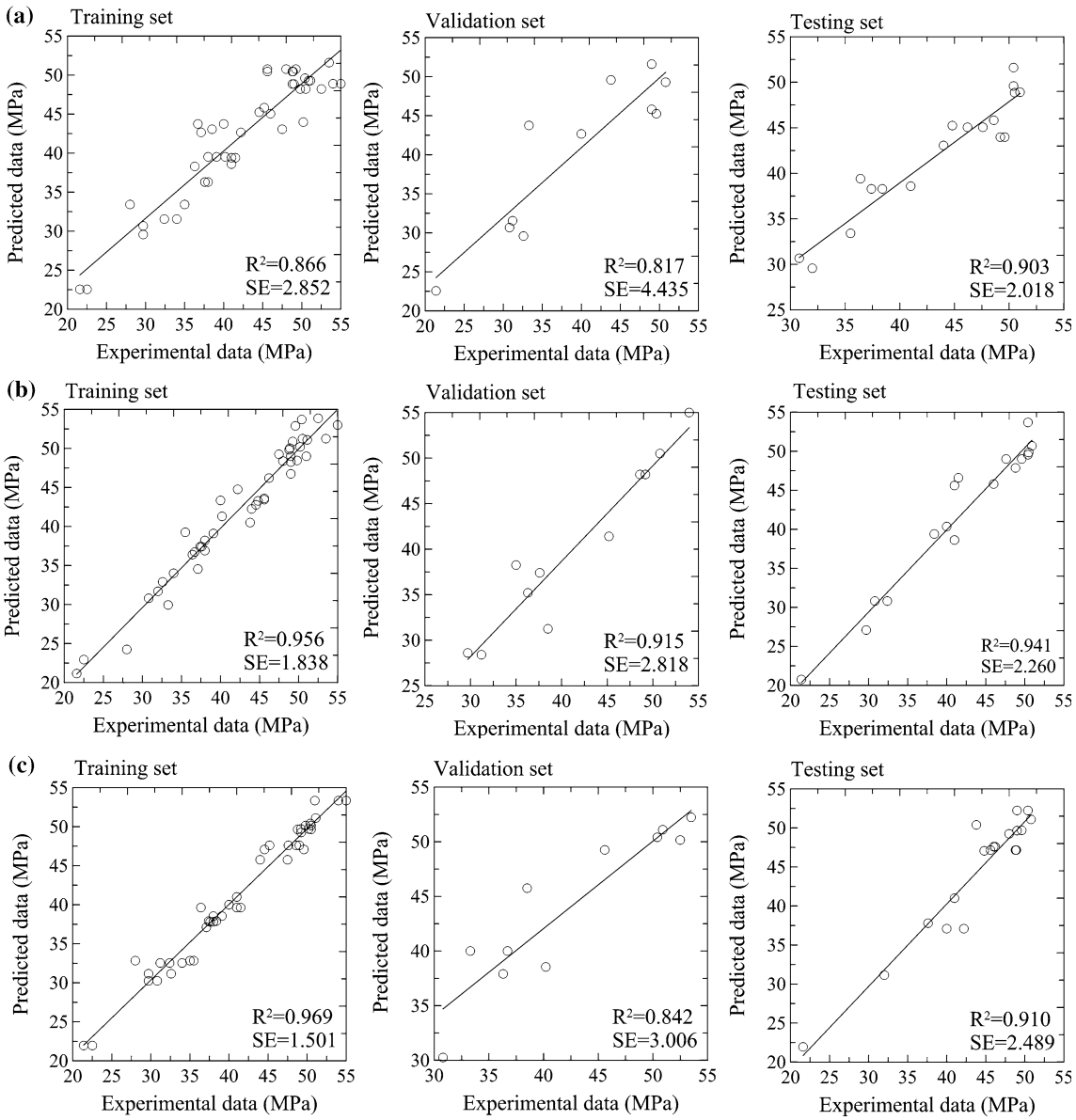

Fig. 2 Comparison of predicted and experimental values of concrete compressive strength (MPa) for training, validation and testing sets, including: **a** 2, **b** 6 and **c** 9 hidden nodes. Training of ANN model was performed using Levenberg–Marquardt learning algorithm. It is clear that ANN with six hidden nodes gives the most accurate predictions that fall within the 95 % prediction interval

thus getting the lowest computational cost. This algorithm is error tolerant, yields good solutions and converges in a small number of iterations [48]. The computational advantage of BFGS especially holds for small- to moderate-sized problems, which is the case in the present analysis. The ANN model with BFGS learning algorithm and different number of hidden nodes is developed for the step length in the range $[10^{-6}, 10^{2}]$, while change in step size takes values from the realm [0.1, 0.5]. Initial step size in interval location step is set to 0.01, while scale factor that determines sufficiently large step size is assumed to be 0.1. Parameter to avoid small reductions in performance is set to 0.1.

As in the previous two models, decrease of MSE with the increase of epochs for training, validation and testing data using different number of hidden nodes excludes the possibility of overfitting (Fig. 5).

Comparison of prediction results with experimental data for training, validation and testing sets, using ANNs with 2, 6, and 9 hidden nodes, is given in Fig. 6. ANN model with nine hidden nodes has the highest coefficient of determination ($R^2 \approx 0.951$) for testing set, approximately the same

Table 8 Comparison of experimental values of concrete compressive strength and predicted data using ANN with Levenberg–Marquardt learning algorithm and six hidden nodes

Sample	Exp. σ_p (MPa)	Pred. σ_p (MPa)	Abs. error (MPa)	Rel. error (%)	Sample	Exp. σ_p (MPa)	Pred. σ_p (MPa)	Abs. error (MPa)	Rel. error (%)
Training set					*Validation set*				
A1-1	55	53.00	2	3.64	A1-2	54	55.00	1	1.85
A1-3	51	49.00	2	3.92	A4-2	36.3	35.20	1.1	3.03
A2-1	45.6	43.58	2.02	4.43	A1-5	48.6	48.20	0.4	0.82
A2-2	49.25	50.88	1.63	3.31	A1-6	45.2	41.40	3.8	8.41
A2-3	48	48.38	0.38	0.79	A2-4	50.8	50.50	0.3	0.59
A3-3	46.2	46.20	0	0.00	A4-6	29.7	28.60	1.1	3.70
A4-1	37.4	37.40	0	0.00	A4-8	37.6	37.40	0.2	0.53
A5-2	53.5	51.25	2.25	4.21	A2-11	38.5	31.25	7.25	18.83
A5-3	49	46.75	2.25	4.59	A5-12	49.2	48.20	1	2.03
A1-4	49	49.00	0	0.00	A1-13	35	38.25	3.25	9.29
A2-6	51.1	51.10	0	0.00	A3-13	31.2	28.40	2.8	8.97
A3-4	38	36.90	1.1	2.89	*Testing set*				
A3-5	39.1	39.10	0	0.00	A3-1	47.6	49.00	1.4	2.94
A3-6	40.2	41.30	1.1	2.74	A3-2	46	45.80	0.2	0.43
A4-5	30.8	30.80	0	0.00	A4-3	38.4	39.40	1	2.60
A5-5	43.8	40.50	3.3	7.53	A5-1	50.4	49.55	0.85	1.69
A5-6	50.4	53.70	3.3	6.55	A2-5	50.9	50.70	0.2	0.39
A1-7	52.5	53.85	1.35	2.57	A4-4	30.8	30.80	0	0.00
A1-9	49.8	48.45	1.35	2.71	A5-4	50.4	53.70	3.3	6.55
A2-7	48.9	50.03	1.13	2.31	A1-8	50.5	49.85	0.65	1.29
A2-8	45.6	43.43	2.17	4.76	A5-8	48.8	47.85	0.95	1.95
A2-9	48.8	49.83	1.03	2.11	A3-10	41	38.63	2.37	5.78
A3-7	36.7	36.73	0.03	0.08	A3-11	41	38.63	2.37	5.78
A3-8	33.3	29.93	3.37	10.12	A3-12	41	38.63	2.37	5.78
A3-9	40	43.33	3.33	8.33	A4-12	29.7	27.10	2.6	8.75
A4-7	38	38.20	0.2	0.53	A5-11	49.6	49.00	0.6	1.21
A4-9	37.6	37.40	0.2	0.53	A2-14	41	45.60	4.6	11.22
A5-7	49	48.25	0.75	1.53	A2-15	41.5	46.60	5.1	12.29
A5-9	50.5	51.25	0.75	1.49	A3-14	32.4	30.80	1.6	4.94
A1-10	49.6	52.88	3.28	6.61	A4-14	21.4	20.75	0.65	3.04
A1-11	44.55	42.78	1.77	3.97	A5-13	40	40.35	0.35	0.88
A1-12	44.8	43.28	1.52	3.39					
A2-10	47.5	49.25	1.75	3.68					
A2-12	44	42.25	1.75	3.98					
A4-10	32	31.70	0.3	0.94					
A4-11	32.6	32.90	0.3	0.92					
A5-10	50.2	50.20	0	0.00					
A1-14	28	24.25	3.75	13.39					
A1-15	35.5	39.25	3.75	10.56					
A2-13	36.4	36.40	0	0.00					
A3-15	34	34.00	0	0.00					
A4-13	21.6	21.15	0.45	2.08					
A4-15	22.5	22.95	0.45	2.00					
A5-14	37.1	34.55	2.55	6.87					

Table 8 continued

Sample	Exp. σ_p (MPa)	Pred. σ_p (MPa)	Abs. error (MPa)	Rel. error (%)	Sample	Exp. σ_p (MPa)	Pred. σ_p (MPa)	Abs. error (MPa)	Rel. error (%)
A5-15	42.2	44.75	2.55	6.04					

Exp. σ_p stands for experimental values of compressive strength, Pred. σ_p for predicted values of compressive strength, Abs. error for absolute error and Rel. error for relative error

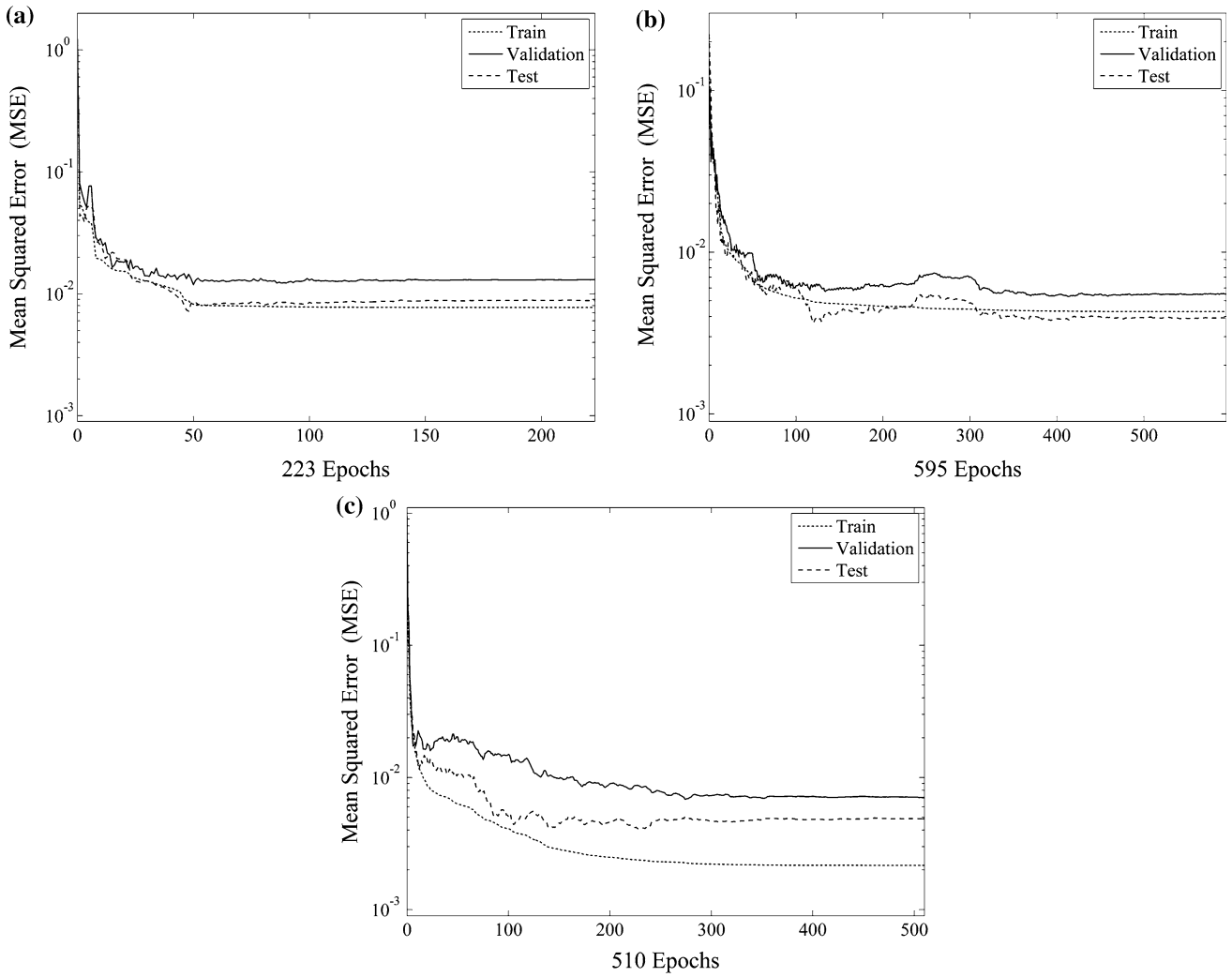

Fig. 3 MSE versus the number of epochs for training, validation and testing data, using different number of hidden nodes: **a** 2, **b** 6 and **c** 9. MSE saturates with the increase of training epochs for both training and validation sets, excluding the possibility of overfitting

value of R^2 for training and validation sets and with statistically small value of standard error, SE = 2.028, meaning that all of the predicted data fall within the 95 % prediction interval, which confirms the precision of the proposed model. Analysis of the error distribution for training, validation and testing sets (for ANN with nine hidden nodes) shows that all of the predicted values for testing set have relative errors smaller than 10 % (Table 10).

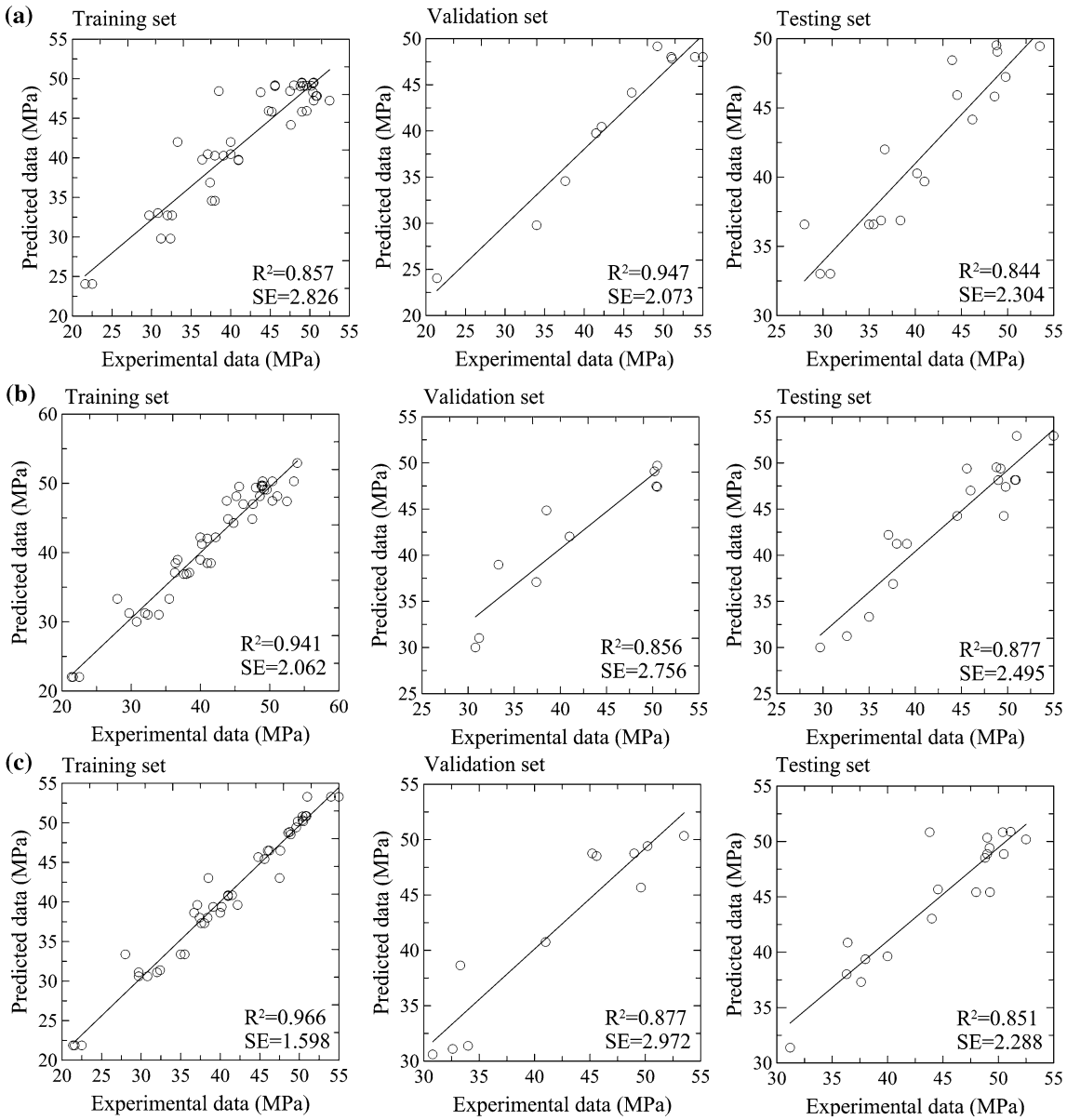

Fig. 4 Comparison of predicted and experimental values of concrete compressive strength (MPa) for training, validation and testing sets, including: **a** 2, **b** 6 and **c** 9 hidden nodes. Training of ANN model was performed using scaled conjugate gradient learning algorithm. It is clear that ANN with six hidden nodes gives the most accurate predictions that fall within the 95 % prediction interval

4.4 One-step-secant (OSS) back-propagation learning algorithm

OSS learning algorithm represents an attempt to bridge the gap between the conjugate gradient and the quasi-Newton secant algorithms. The OSS method does not require the choice of critical parameters, is guaranteed to converge to a point with zero gradient, and has been shown to accelerate the learning phase by many orders of magnitude with respect to standard back-propagation algorithms if high precision in the output values is desired [49]. In the present study, parameters for OSS learning algorithm are the same as for the previous BFGS method.

MSE versus the number of epochs for training, validation and testing data, using different number of hidden nodes, is shown in Fig. 7. The results of all three models are reasonable, since the training set errors and the validation set errors have similar properties. Consequently, it does not appear that any significant overfitting has occurred.

Table 9 Comparison of experimental values of concrete compressive strength and predicted data using ANN with scaled conjugate gradient learning algorithm and six hidden nodes

Sample	Exp. σ_p (MPa)	Pred. σ_p (MPa)	Abs. error (MPa)	Rel. error (%)	Sample	Exp. σ_p (MPa)	Pred. σ_p (MPa)	Abs. error (MPa)	Rel. error (%)
Training set					*Validation set*				
A1-2	54	52.93	1.07	1.97	A4-1	37.4	37.09	0.31	0.82
A2-3	48	49.39	1.39	2.89	A4-4	30.8	30.01	0.79	2.57
A3-1	47.6	47.01	0.59	1.25	A5-6	50.4	47.48	2.92	5.80
A3-3	46.2	47.01	0.81	1.75	A1-8	50.5	47.41	3.09	6.12
A4-2	36.3	37.09	0.79	2.18	A3-8	33.3	38.97	5.67	17.00
A4-3	38.4	37.09	1.31	3.41	A5-9	50.5	49.70	0.80	1.59
A5-1	50.4	50.29	0.11	0.22	A2-11	38.5	44.85	6.35	16.49
A5-2	53.5	50.29	3.21	6.01	A3-11	41	42.03	1.03	2.51
A5-3	49	50.29	1.29	2.63	A3-12	41	42.03	1.03	2.51
A1-5	48.6	48.14	0.46	0.95	A5-10	50.2	49.10	1.10	2.20
A1-6	45.2	48.14	2.94	6.50	A3-13	31.2	31.02	0.18	0.58
A2-6	51.1	48.16	2.94	5.76	*Testing set*				
A3-6	40.2	41.24	1.04	2.59	A1-1	55	52.93	2.07	3.75
A4-5	30.8	30.01	0.79	2.57	A1-3	51	52.93	1.93	3.79
A5-4	50.4	47.48	2.92	5.80	A2-1	45.6	49.39	3.79	8.31
A5-5	43.8	47.48	3.68	8.39	A2-2	49.25	49.39	0.14	0.28
A1-7	52.5	47.41	5.09	9.70	A3-2	46	47.01	1.01	2.19
A2-7	48.9	49.53	0.63	1.29	A1-4	49	48.14	0.86	1.76
A2-8	45.6	49.53	3.93	8.62	A2-4	50.8	48.16	2.64	5.21
A3-7	36.7	38.97	2.27	6.18	A2-5	50.9	48.16	2.74	5.39
A3-9	40	38.97	1.03	2.58	A3-4	38	41.24	3.24	8.53
A4-7	38	36.90	1.10	2.90	A3-5	39.1	41.24	2.14	5.47
A4-8	37.6	36.90	0.70	1.87	A4-6	29.7	30.01	0.31	1.04
A5-7	49	49.70	0.70	1.43	A1-9	49.8	47.41	2.39	4.80
A5-8	48.8	49.70	0.90	1.84	A2-9	48.8	49.53	0.73	1.50
A1-12	44.8	44.27	0.53	1.19	A4-9	37.6	36.90	0.70	1.87
A2-10	47.5	44.85	2.65	5.58	A1-10	49.6	44.27	5.33	10.75
A2-12	44	44.85	0.85	1.93	A1-11	44.55	44.27	0.28	0.63
A3-10	41	42.03	1.03	2.51	A4-11	32.6	31.24	1.36	4.16
A4-10	32	31.24	0.76	2.36	A1-13	35	33.32	1.68	4.80
A4-12	29.7	31.24	1.54	5.20	A5-14	37.1	42.20	5.10	12.09
A5-11	49.6	49.10	0.50	1.02					
A5-12	49.2	49.10	0.10	0.21					
A1-14	28	33.32	5.32	19.00					
A1-15	35.5	33.32	2.18	6.14					
A2-13	36.4	38.47	2.07	5.68					
A2-14	41	38.47	2.53	6.17					
A2-15	41.5	38.47	3.03	7.30					
A3-14	32.4	31.02	1.38	4.26					
A3-15	34	31.02	2.98	8.76					
A4-13	21.6	22.03	0.43	1.99					
A4-14	21.4	22.03	0.63	2.94					
A4-15	22.5	22.03	0.47	2.09					
A5-13	40	42.20	2.20	5.51					
A5-15	42.2	42.20	0.00	0.01					

Exp. σ_p stands for experimental values of compressive strength, Pred. σ_p for predicted values of compressive strength, Abs. error for absolute error and Rel. error for relative error

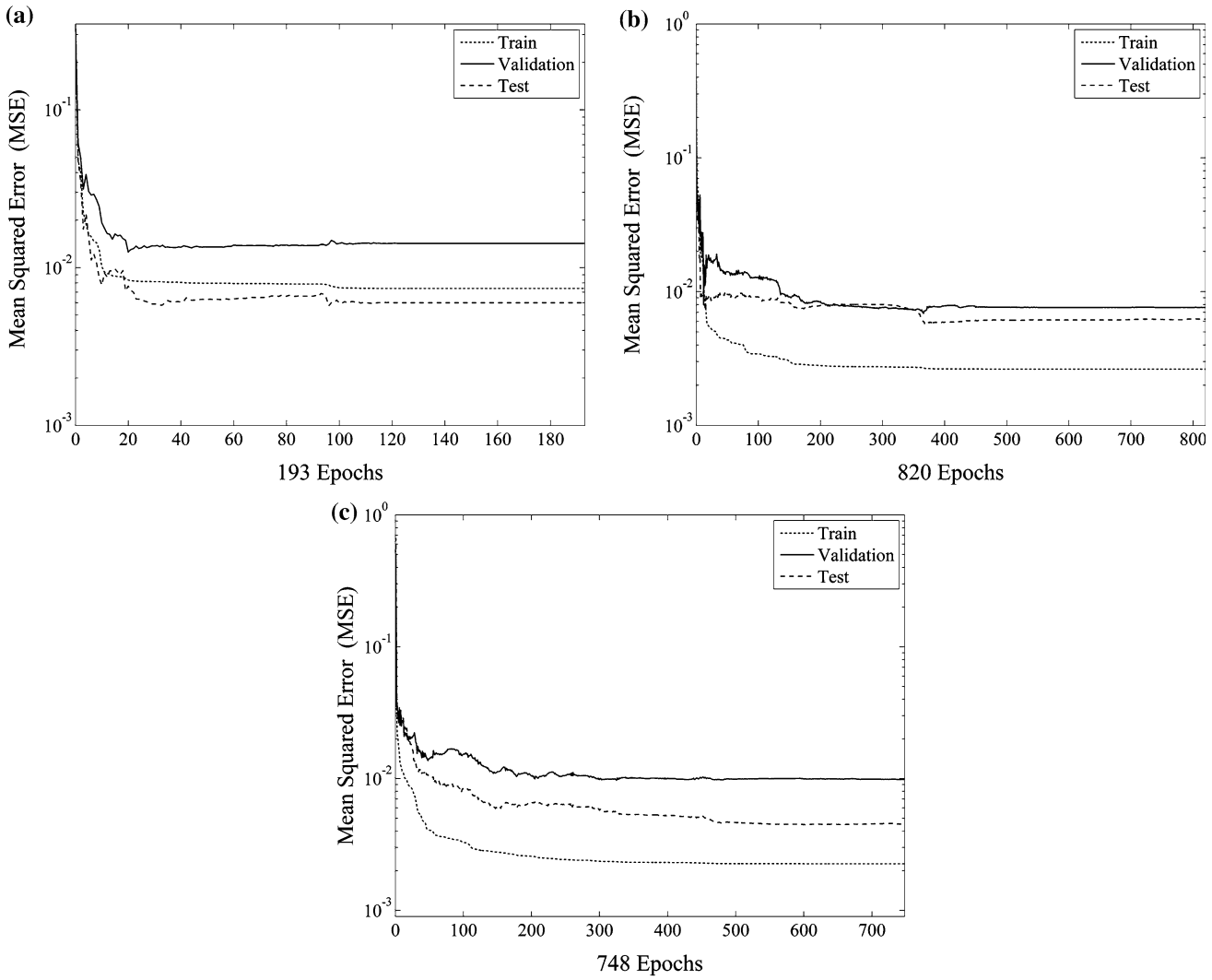

Fig. 5 MSE versus the number of epochs for training, validation and testing data, using different number of hidden nodes: **a** 2, **b** 6 and **c** 9. MSE saturates with the increase of training epochs for both training and validation set, excluding the possibility of overfitting

Comparison of prediction results with experimental data for training, validation and testing sets, using ANNs with 2, 6, and 9 hidden nodes, is given in Fig. 8. ANN model with six hidden nodes has the highest coefficient of determination ($R^2 \approx 0.951$) for testing set, approximately the same value of R^2 for training set and with statistically small value of standard error, SE = 2.028, meaning that all of the predicted data fall within the 95 % prediction interval, which confirms the precision of the proposed model. Slightly lower value of R^2 for validation set does not affect the obtained results significantly, since standard error indicates that predicted data fall within the 95 % prediction interval (SE = 3.193). Analysis of the error distribution for training, validation and testing sets (for ANN with six hidden nodes) shows that relative prediction errors are up to $\approx$10 % (Table 11).

5 Performance evaluation of the proposed models

Performances of the developed prediction models could be further evaluated using different standard statistical criteria given in Table 12 [50].

Calculated statistical errors are shown in Table 13. ANN model with OSS learning algorithm and six hidden nodes has the lowest values of MAPE (Mean Absolute Percentage Error) and VARE (Variance Absolute Relative Error), while model with LM learning algorithm and six hidden

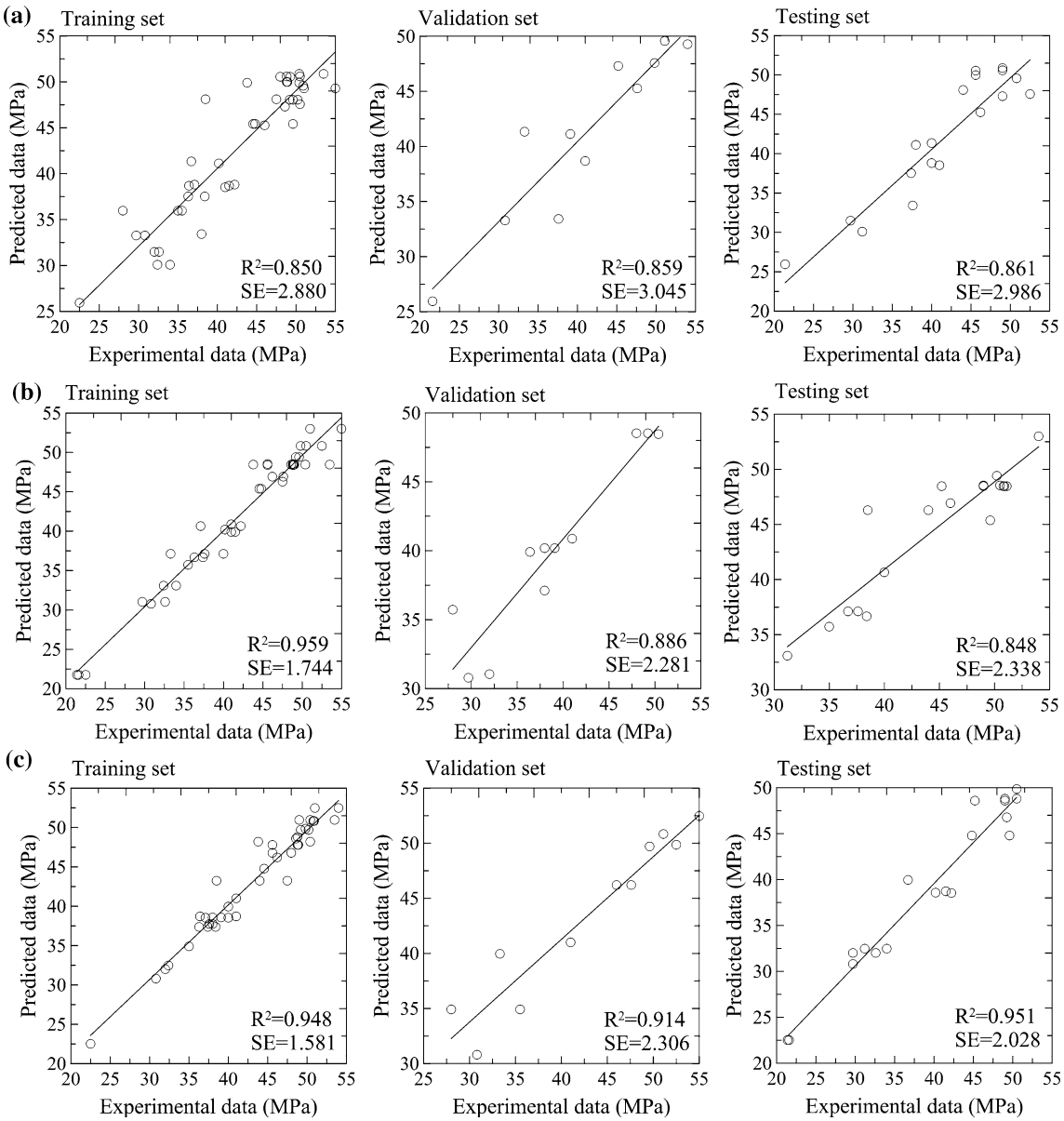

Fig. 6 Comparison of predicted and experimental values of concrete compressive strength (MPa) for training, validation and testing sets, including: **a** 2, **b** 6 and **c** 9 hidden nodes. Training of ANN model was performed using BFGS learning algorithm. It is clear that ANN with six hidden nodes gives the most accurate predictions that fall within the 95 % prediction interval

nodes has the lowest value of and MEDAE (MEDian Absolute Error), in comparison with other proposed ANN models.

6 Sensitivity analysis

Sensitivity analysis represents a method which enables us to determine the relative strength of effect (RSE) for each input unit on the concrete compressive strength [51]. In this case, it was carried out by the hierarchical analysis [52], where the RSE parameter is determined in the following way:

$$\mathrm{RSE}_{ki} = C \sum_{jn} \sum_{jn-1} \cdots \sum_{j1} W_{j_n k} G(e_k) W_{j_{n-1} j_n} G\left(e_{j_n}\right) \times W_{j_{n-2} j_{n-1}} G\left(e_{j_{n-1}}\right) W_{j_{n-3} j_{n-2}} G\left(e_{j_{n-2}}\right) \cdots W_{i j_1} G\left(e_{j_1}\right), \quad (2)$$

Table 10 Comparison of experimental values of concrete compressive strength and predicted data using ANN with BFGS learning algorithm and nine hidden nodes

Sample	Exp. σ_p (MPa)	Pred. σ_p (MPa)	Abs. error (MPa)	Rel. error (%)	Sample	Exp. σ_p (MPa)	Pred. σ_p (MPa)	Abs. error (MPa)	Rel. error (%)
Training set					*Validation set*				
A1-2	54	52.47	1.53	2.83	A1-1	55	52.47	2.53	4.59
A1-3	51	52.47	1.47	2.89	A3-1	47.6	46.20	1.40	2.93
A2-1	45.6	46.78	1.18	2.59	A3-2	46	46.20	0.20	0.44
A2-3	48	46.78	1.22	2.54	A2-6	51.1	50.83	0.27	0.54
A3-3	46.2	46.20	0.00	0.01	A4-4	30.8	30.80	0.00	0.01
A4-1	37.4	37.36	0.04	0.10	A1-7	52.5	49.86	2.64	5.03
A4-2	36.3	37.36	1.06	2.93	A3-8	33.3	39.96	6.66	19.99
A4-3	38.4	37.36	1.04	2.70	A3-12	41	41.00	0.00	0.01
A5-1	50.4	50.96	0.56	1.12	A5-11	49.6	49.71	0.11	0.22
A5-2	53.5	50.96	2.54	4.74	A1-14	28	34.91	6.91	24.68
A5-3	49	50.96	1.96	4.01	A1-15	35.5	34.91	0.59	1.66
A1-5	48.6	48.59	0.01	0.01	*Testing set*				
A2-4	50.8	50.83	0.03	0.05	A2-2	49.25	46.78	2.47	5.01
A2-5	50.9	50.83	0.07	0.15	A1-4	49	48.59	0.41	0.83
A3-4	38	38.57	0.57	1.49	A1-6	45.2	48.59	3.39	7.51
A3-5	39.1	38.57	0.53	1.36	A3-6	40.2	38.57	1.63	4.06
A4-5	30.8	30.80	0.00	0.01	A4-6	29.7	30.80	1.10	3.72
A5-4	50.4	48.19	2.21	4.38	A1-8	50.5	49.86	0.64	1.27
A5-5	43.8	48.19	4.39	10.03	A3-7	36.7	39.96	3.26	8.88
A5-6	50.4	48.19	2.21	4.38	A5-7	49	48.80	0.20	0.40
A1-9	49.8	49.86	0.06	0.11	A5-9	50.5	48.80	1.70	3.36
A2-7	48.9	47.79	1.11	2.26	A1-10	49.6	44.78	4.82	9.71
A2-8	45.6	47.79	2.19	4.81	A1-12	44.8	44.78	0.02	0.04
A2-9	48.8	47.79	1.01	2.06	A4-11	32.6	32.01	0.59	1.80
A3-9	40	39.96	0.04	0.10	A4-12	29.7	32.01	2.31	7.79
A4-7	38	37.74	0.26	0.67	A2-15	41.5	38.72	2.78	6.71
A4-8	37.6	37.74	0.14	0.38	A3-13	31.2	32.47	1.27	4.07
A4-9	37.6	37.74	0.14	0.38	A3-15	34	32.47	1.53	4.50
A5-8	48.8	48.80	0.00	0.00	A4-13	21.6	22.52	0.92	4.28
A1-11	44.55	44.78	0.23	0.52	A4-14	21.4	22.52	1.12	5.25
A2-10	47.5	43.25	4.25	8.94	A5-15	42.2	38.54	3.66	8.67
A2-11	38.5	43.25	4.75	12.34					
A2-12	44	43.25	0.75	1.70					
A3-10	41	41.00	0.00	0.01					
A3-11	41	41.00	0.00	0.01					
A4-10	32	32.01	0.01	0.04					
A5-10	50.2	49.71	0.49	0.98					
A5-12	49.2	49.71	0.51	1.03					
A1-13	35	34.91	0.09	0.26					
A2-13	36.4	38.72	2.32	6.36					
A2-14	41	38.72	2.28	5.57					
A3-14	32.4	32.47	0.07	0.22					
A4-15	22.5	22.52	0.02	0.10					
A5-13	40	38.54	1.46	3.64					
A5-14	37.1	38.54	1.44	3.89					

Exp. σ_p stands for experimental values of compressive strength, Pred. σ_p for predicted values of compressive strength, Abs. error for absolute error and Rel. error for relative error

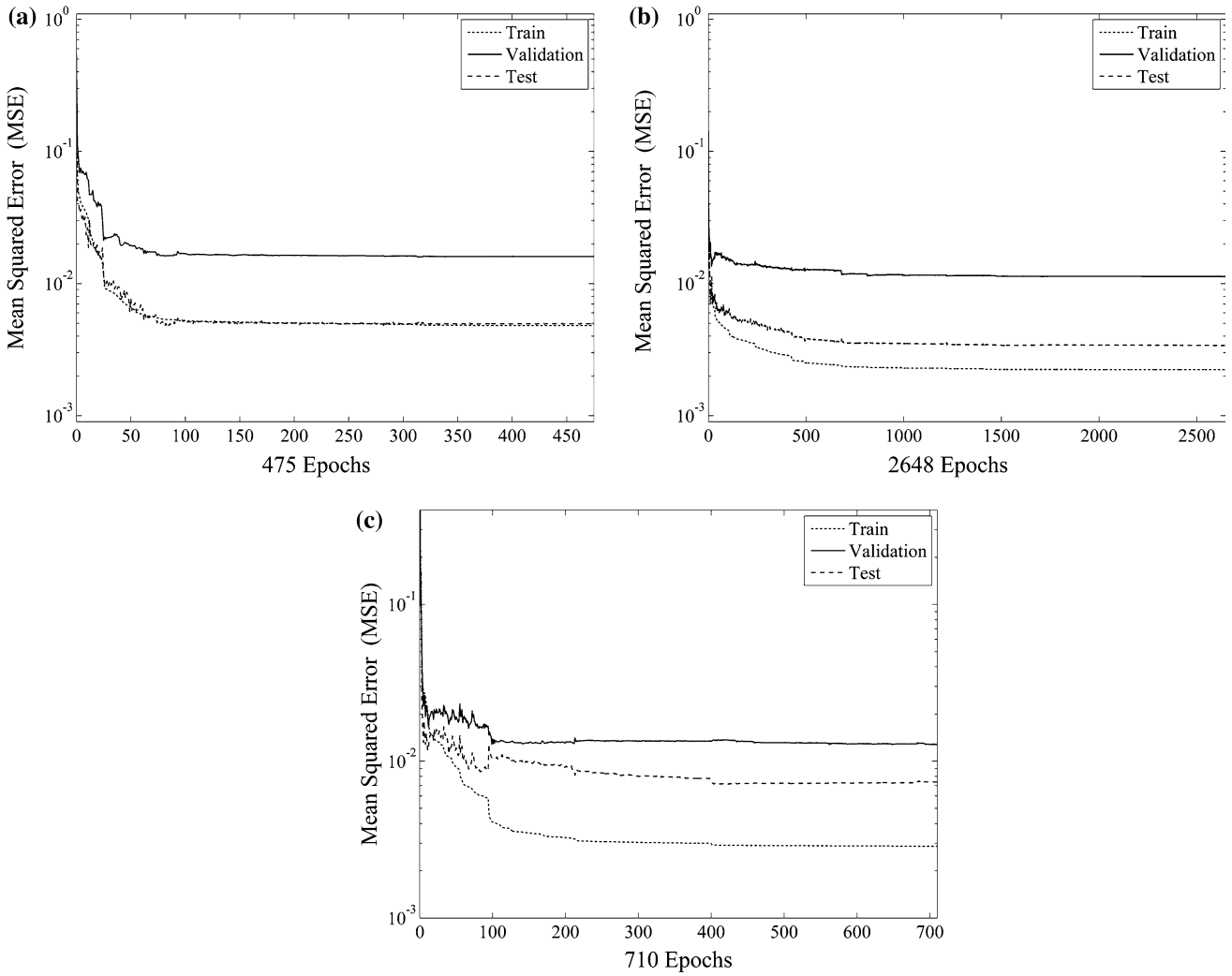

Fig. 7 MSE versus the number of epochs for training, validation and testing data, using different number of hidden nodes: **a** 2, **b** 6 and **c** 9. MSE saturates with the increase of training epochs for both training and validation sets, excluding the possibility of overfitting

where C is normalized constant which controls the maximum absolute values of RSE_{ki}, W is a connected weight and $G(e_k) = \exp(-e_k)/(1+\exp(-e_k))^2$ denotes the hidden units in the n, $n-1$, $n-2$,…,1 hidden layers [52].

Global sensitivity analysis, which was carried out for all the input parameters and for all the ANN models with different learning algorithms and different number of hidden nodes, indicated that the *w*/*c* ratio has the strongest impact on the compressive strength of concrete (Fig. 9).

7 Conclusion

In the present study, we develop four ANN models with different learning algorithms for prediction of concrete compressive strength. For this purpose, 75 specimens of basic concrete mixture were exposed to different cycles of freezing and thawing, after which their compressive strength was measured at different ages (7, 20 and 32 days). Afterward, these results were used for ANN modeling with different number of hidden nodes in order to exclude the possibility of overfitting. In all the examined cases, a three-layer feed-forward back-propagation artificial neural network was used. The obtained results showed that ANN models with six hidden nodes (using LM, SCG and OSS learning algorithms) and nine hidden nodes (using BFGS learning algorithm) have the best predictive power comparable to the experimental results. Moreover, in all the examined cases, analysis of standard error indicated that each predicted value falls within the 95 % prediction interval. As for the error distribution, further inquiry implied that relative

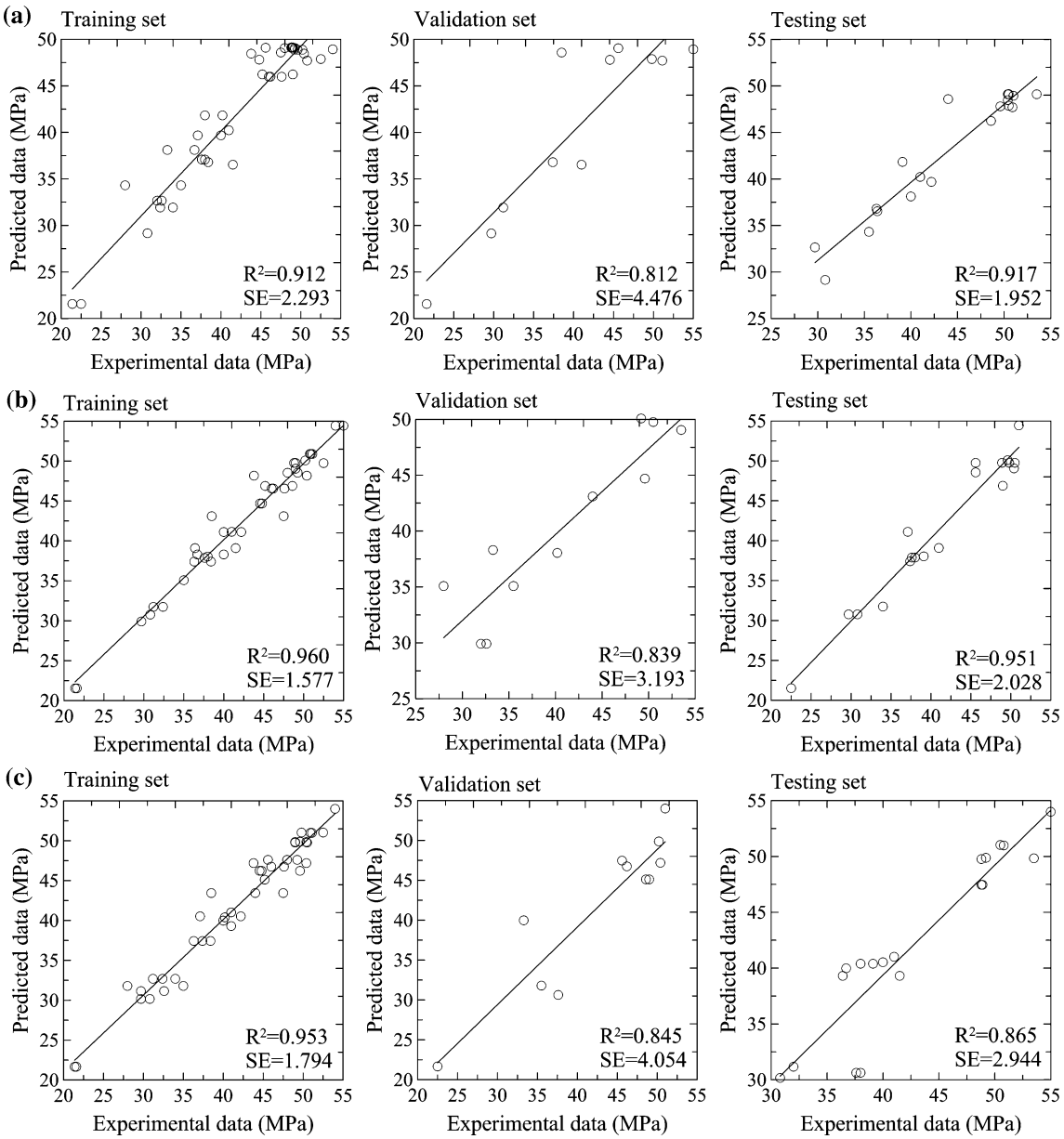

Fig. 8 Comparison of predicted and experimental values of concrete compressive strength (MPa) for training, validation and testing sets, including: **a** 2, **b** 6 and **c** 9 hidden nodes. Training of ANN model was performed using OSS learning algorithm. It is clear that ANN with six hidden nodes gives the most accurate predictions that fall within the 95 % prediction interval

Table 11 Comparison of experimental values of concrete compressive strength and predicted data using ANN with OSS learning algorithm and six hidden nodes

Sample	Exp. σ_p (MPa)	Pred. σ_p (MPa)	Abs. error (MPa)	Rel. error (%)	Sample	Exp. σ_p (MPa)	Pred. σ_p (MPa)	Abs. error (MPa)	Rel. error (%)
Training set					*Validation set*				
A1-1	55	54.45	0.55	1.01	A5-2	53.5	49.06	4.44	8.30
A1-2	54	54.45	0.45	0.82	A3-6	40.2	38.04	2.16	5.37
A2-2	49.25	48.55	0.70	1.42	A3-8	33.3	38.31	5.01	15.04
A2-3	48	48.55	0.55	1.15	A5-9	50.5	49.77	0.73	1.45
A3-1	47.6	46.57	1.03	2.16	A1-10	49.6	44.69	4.91	9.89

Table 11 continued

Sample	Exp. σ_p (MPa)	Pred. σ_p (MPa)	Abs. error (MPa)	Rel. error (%)	Sample	Exp. σ_p (MPa)	Pred. σ_p (MPa)	Abs. error (MPa)	Rel. error (%)
A3-2	46	46.57	0.57	1.24	A2-12	44	43.10	0.90	2.05
A3-3	46.2	46.57	0.37	0.81	A4-10	32	29.91	2.09	6.53
A4-2	36.3	37.41	1.11	3.06	A4-11	32.6	29.91	2.69	8.25
A4-3	38.4	37.41	0.99	2.58	A5-12	49.2	50.08	0.88	1.79
A5-3	49	49.06	0.06	0.12	A1-14	28	35.08	7.08	25.28
A1-5	48.6	46.88	1.72	3.53	A1-15	35.5	35.08	0.42	1.18
A1-6	45.2	46.88	1.68	3.73	*Testing set*				
A2-4	50.8	50.91	0.11	0.21	A1-3	51	54.45	3.45	6.76
A2-5	50.9	50.91	0.01	0.01	A2-1	45.6	48.55	2.95	6.48
A2-6	51.1	50.91	0.19	0.38	A4-1	37.4	37.41	0.01	0.03
A3-4	38	38.04	0.04	0.11	A5-1	50.4	49.06	1.34	2.66
A4-4	30.8	30.78	0.02	0.06	A1-4	49	46.88	2.12	4.32
A5-4	50.4	48.19	2.21	4.39	A3-5	39.1	38.04	1.06	2.70
A5-5	43.8	48.19	4.39	10.01	A4-5	30.8	30.78	0.02	0.06
A5-6	50.4	48.19	2.21	4.39	A4-6	29.7	30.78	1.08	3.65
A1-7	52.5	49.76	2.74	5.22	A1-8	50.5	49.76	0.74	1.46
A2-9	48.8	49.77	0.97	1.99	A1-9	49.8	49.76	0.04	0.08
A3-7	36.7	38.31	1.61	4.38	A2-7	48.9	49.77	0.87	1.78
A3-9	40	38.31	1.69	4.23	A2-8	45.6	49.77	4.17	9.14
A4-9	37.6	37.88	0.28	0.74	A4-7	38	37.88	0.12	0.32
A5-7	49	49.77	0.77	1.56	A4-8	37.6	37.88	0.28	0.74
A5-8	48.8	49.77	0.97	1.98	A5-11	49.6	50.08	0.48	0.97
A1-11	44.55	44.69	0.14	0.32	A2-14	41	39.09	1.91	4.67
A1-12	44.8	44.69	0.11	0.24	A3-15	34	31.75	2.25	6.63
A2-10	47.5	43.10	4.40	9.27	A4-15	22.5	21.53	0.97	4.29
A2-11	38.5	43.10	4.60	11.94	A5-14	37.1	41.11	4.01	10.82
A3-10	41	41.15	0.15	0.36					
A3-11	41	41.15	0.15	0.36					
A3-12	41	41.15	0.15	0.36					
A4-12	29.7	29.91	0.21	0.71					
A5-10	50.2	50.08	0.12	0.23					
A1-13	35	35.08	0.08	0.23					
A2-13	36.4	39.09	2.69	7.38					
A2-15	41.5	39.09	2.41	5.81					
A3-13	31.2	31.75	0.55	1.75					
A3-14	32.4	31.75	0.65	2.02					
A4-13	21.6	21.53	0.07	0.31					
A4-14	21.4	21.53	0.13	0.63					
A5-13	40	41.11	1.11	2.78					
A5-15	42.2	41.11	1.09	2.58					

Exp. σ_p stands for experimental values of compressive strength, Pred. σ_p for predicted values of compressive strength, Abs. error for absolute error and Rel. error for relative error

Table 12 Statistical error parameters used for models' evaluation

Statistical parameter	Equation
Mean absolute percentage error (MAPE)	$\text{MAPE} = \frac{1}{n} \times \left[\sum_{i=1}^{n} \left\lvert \frac{t_i - x_i}{t_i} \right\rvert \right] \times 100$
Variance absolute relative error (VARE)	$\text{VARE} = \frac{1}{n} \times \left[\sum_{i=1}^{n} \left(\left\lvert \frac{t_i - x_i}{t_i} \right\rvert - \text{mean} \left\lvert \frac{t_i - x_i}{t_i} \right\rvert^2 \right) \right] \times 100$
Median absolute error (MEDAE)	$\text{MEDAE} = \text{median}(t_i - x_i)$

t_i represents measured value of compressive strength, while x_i denotes predicted value of compressive strength

Table 13 Statistical errors of different models for predicting PPV

ANN model		Statistical errors		
Learning algorithm	No. of hidden nodes	MAPE	VARE	MEDAE
Levenberg–Marquardt	6	4.079	4.064	1.000
Scaled gradient descent	6	4.630	4.612	1.930
BFGS	9	4.622	4.606	1.530
One-step secant	6	3.555	3.544	1.060

prediction error increases up to the acceptable value of ≈ 15 %, which suggests that the proposed ANN models are robust to the consistency of the training and validation data. Additional analysis indicated that ANN model with OSS learning algorithm and six hidden nodes has the lowest values of MAPE and VARE, while the model with LM algorithm and six nodes has the lowest value of MEDAE.

Regarding the separate impact of each input unit on the final value of concrete compressive strength, the sensitivity analysis indicated that *w/c* ratio has the strongest influence on the experimental results in all the examined cases with various learning algorithms and different number of hidden nodes.

It should be noted that one of the main outcome of the performed analysis lies in the fact that the results of ANN modeling seem to be almost independent on the choice of learning algorithm and number of hidden nodes (as long as this number is in the acceptable range determined by the widely used heuristics). This claim follows the results of ANN training in all the examined cases, with high coefficient of determination for every training, validation and testing sets ($R^2 > 0.81$). This fact is further supported by the low values of SE and favorable change of MSE with the number of training epochs.

However, despite the high predictive power of the proposed ANN models, one of the main limitations of the analysis is certainly simple composition of the concrete

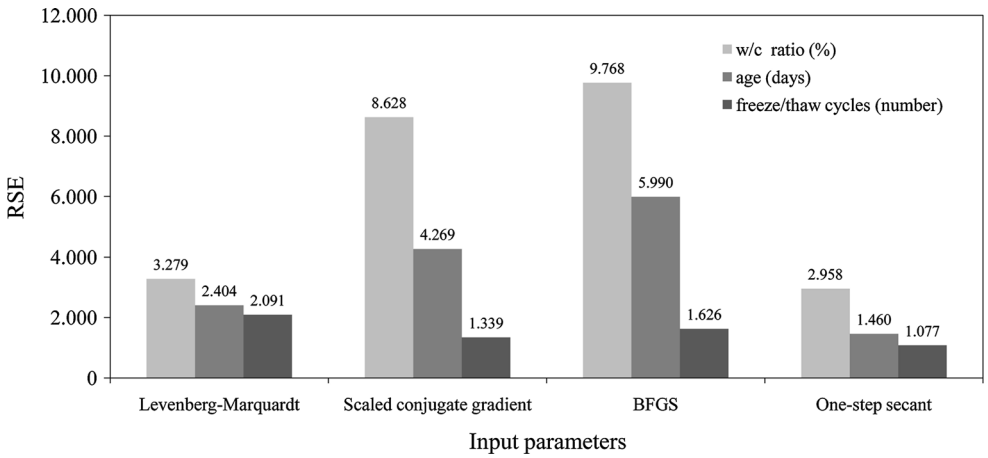

Fig. 9 Relative strength of effect (RSE) of each input parameter on the recorded value of concrete compressive strength, as a result of global sensitivity analysis, for ANN model with LM learning algorithm and six hidden nodes, SCG learning algorithm and six hidden nodes, BFGS learning algorithm and nine hidden nodes and OSS learning algorithm and six hidden nodes

specimens. Future analyzes should include concrete samples with different additives (superplasticizer, fly ash, zeolite, etc.), in order to expand the proposed models and make them more usable in daily practice.

Acknowledgments This research was partly supported by the Ministry of Education, Science and Technological Development of the Republic of Serbia (No. 176016). Special thanks go to Tomislav Vasović for thorough participation in the experimental part of the performed research.

References

1. Saul AGA (1951) Principles underlying the steam curing of concrete at atmospheric pressure. Mag Concr Res 2:127–140
2. Plowman JM (1956) Maturity and the strength of concrete. Mag Concr Res 22:13–22
3. Bernhardt CJ (1956) Hardening of concrete at different temperatures. In: RILEM symposium on winter concreting, Copenhagen, Danish Institute for Building Research, Session B-II
4. Yi S-T, Moon Y-H, Kim J-K (2005) Long-term strength prediction of concrete with curing temperature. Cem Concr Res 35:1961–1969
5. Popovics S, Ujhelyi J (2008) Contribution to the concrete strength versus water-cement ratio relationship. J Mater Civ Eng 20:459–463
6. Sobhani J, Najimi M, Pourkhorshidi AR, Parhizkar T (2010) Prediction of the compressive strength of no-slump concrete: a comparative study of regression, neural network and ANFIS models. Constr Build Mater 24:709–718
7. Ramezanianpour AA, Sobhani M, Sobhani J (2004) Application of network based neuro-fuzzy system for prediction of the strength of high strength concrete. AMIRKABIR 15:78–93
8. Saridemir M (2009) Predicting the compressive strength of mortars containing metakaolin by artificial neural networks and fuzzy logic. Adv Eng Softw 40:920–927
9. Topcu IB, Saridemir M (2008) Prediction of compressive strength of concrete containing fly ash using artificial neural networks and fuzzy logic. Comput Mater Sci 41:305–311
10. Singh R, Vishal V, Singh TN, Ranjith PG (2012) A comparative study of generalized regression neural network approach and adaptive neuro-fuzzy inference systems for prediction of unconfined compressive strength of rocks. Neural Comp Appl 23:499–506
11. Singh R, Vishal V, Singh TN (2012) Soft computing method for assessment of compressional wave velocity. Sci Iran 19:1018–1024
12. Basyigit C, Akkurt I, Kilincarslan S, Beycioglu A (2010) Prediction of compressive strength of heavyweight concrete by ANN and FL models. Neural Comp Appl 19:507–513
13. Basma AA, Barakat S, Oraimi SA (1999) Prediction of cement degree of hydration using artificial neural networks. Mater J 96:166–172
14. Jepsen MT (2002) Predicting concrete durability by using artificial neural network. Special NCR-publication; ID 5268
15. Graham LD, Forbes DR, Smith SD (2006) Modeling the ready mixed concrete delivery system with neural network. Autom Constr 15:656–663
16. Lai S, Serra M (1997) Concrete strength prediction by means of neural network. Constr Build Mater 11:93–98
17. Yeh I (1998) Modeling of strength of high-performance concrete using artificial neural networks. Cem Concr Res 28:1797–1808
18. Oh J-W, Lee I-W, Kim J-T, Lee G-W (1999) Application of neural networks for proportioning of concrete. Mater J 96:352–356
19. Dias W, Pooliyadda S (2001) Neural network for predicting properties of concretes with admixtures. Constr Build Mater 15:371–379
20. Lee S-C (2003) Prediction of concrete strength using artificial neural networks. Eng Struct 25:849–857
21. Kim JI, Kim DK, Feng MQ, Yazdani F (2004) Application of neural networks for estimation of concrete strength. J Mater Civ Eng 16:257–264
22. Gupta R, Kewalramani MA, Goel A (2006) Prediction of concrete strength using neural-expert system. ASCE J Mater Civ Eng 18:462–466
23. Oztas A, Pala M, Ozbay E, Kanca E, Caglar N, Bhatti MA (2006) Predicting the compressive strength and slump of high strength concrete using neural network. Constr Build Mater 20:769–775
24. Bai J, Wild S, Ware JA, Sabir BB (2003) Using neural networks to predict workability of concrete. Adv Eng Softw 34:663–669
25. Mukherjee A, Biswas SN (1997) Artificial neural networks in prediction of mechanical behavior of concrete at high temperature. Nucl Eng Des 178:1–11
26. Pala M, Ozbay E, Oztas A, Yuce MI (2007) Appraisal of long-term effects of fly ash and silica fume on compressive strength of concrete by neural networks. Constr Build Mater 21:384–394
27. SRPS ISO 2736-1:1997. Concrete tests—test specimens—part 1: sampling of fresh concrete
28. SRPS ISO 2736-2:1997. Concrete tests—test specimens—part 2: making and curing of test specimens for strength tests
29. SRPS ISO 4109:1997. Fresh concrete—determination of the consistency—slump test
30. SRPS ISO 4110:1997. Fresh concrete—determination of the consistency—Vebe test
31. SRPS U.M8.052:1996. Fresh concrete—determination of the consistency—flow test
32. SRPS CEN/TR 15177:2009. Testing the freeze–thaw resistance of concrete—internal structural damage
33. Neville A (2002) Properties of concrete, 4th edn. Wiley, New York
34. SRPS EN 12390-3:2010. Testing hardened concrete—part 3: compressive strength of test specimens
35. Yaprak H, Karaci A, Demir I (2013) Prediction of the effect of varying cure conditions and w/c ratio on the compressive strength of concrete using artificial neural networks. Neural Comp Appl 22:133–141
36. Sarkar K, Tiwary A, Singh TN (2010) Estimation of strength parameters of rock using artificial neural networks. Bull Eng Geol Environ 69:599–606
37. Monjezi M, Singh TN, Khandelwal M, Sinha S, Singh V, Hosseini I (2006) Prediction and analysis of blast parameters using artificial neural network. Noise Vib Control Worldw 37:8–16
38. Rumelhart DE, Hinton GE, Williams RJ (1986) Learning internal representation by error propagation. In: Rumelhart DE, McCleland JL (eds) Parallel distribution processing: explorations in the microstructure of cognition, vol 1. MIT Press, Cambridge, pp 318–362
39. Lippmann RP (1987) An introduction to computing with neural nets. IEEE ASSP Mag 4:4–22
40. Sonmez H, Gokceoglu C, Nefeslioglu HA, Kayabasi A (2006) Estimation of rock modulus: for intact rocks with an artificial neural network and for rock masses with a new empirical equation. Int J Rock Mech Min 43:224–235
41. Looney CG (1996) Advances in feed-forward neural networks: demystifying knowledge acquiring black boxes. IEEE Trans Knowl Data Eng 8:211–226
42. Nelson M, Illingworth WT (1990) A practical guide to neural nets. Addison-Wesley, Reading

43. MATLAB Neural Network Toolbox (2014). www.mathworks.com/products/neural-network
44. Khandelwal M, Singh TN (2010) Prediction of macerals contents of Indian coals from proximate and ultimate analyses using artificial neural networks. Fuel 89:1101–1109
45. Singh TN, Kanchan R, Verma AK, Saigal K (2005) A comparative study of ANN and Neuro-fuzzy for the prediction of dynamic constant of rockmass. J Earth Syst Sci 114:75–86
46. Fletcher R (2000) Practical methods of optimization. Wiley, New York
47. Moller MF (1993) A scaled conjugate gradient algorithm for fast supervised learning. Neural Netw 6:525–533
48. Dennis JE, Schnabel RB (1987) Numerical methods for unconstrained optimization and nonlinear equations. Society for industrial and applied mathematics
49. Battiti R (1992) First- and second-order methods for learning: between steepest descent and Newton's method. Neural Comput 4:141–166
50. Monjezi M, Hasanipanah M, Khandelwal M (2013) Evaluation and prediction of blast-induced ground vibration at Shur River Dam, Iran, by artificial neural network. Neural Comput Appl 22:1637–1643
51. Khandelwal M, Singh TN (2009) Prediction of blast-induced ground vibration using artificial neural network. Int J Rock Mech Min 46:1214–1222
52. Yang Y, Zang O (1997) A hierarchical analysis for rock engineering using artificial neural networks. Rock Mech Rock Eng 30:207–222